BehavioralSimulation of a Non-resonant MEMS Gyro-accelerometer

PayalVerma[1], R. Gopal[1], Sandeep K. Arya[2]

[1]*MEMS & Micro-sensor Group, CSIR-Central Electronics Engineering Research Institute, Pilani, Rajasthan, 333 031, India.*
[2]*Department of Electronics and Communication Engineering, Guru Jambheshwar University of Science and Technology, Hisar, Haryana,125001, India*

***Abstract*—** Behavioral level simulations are a quick and efficient (reliable) technique to analyze the behavior of complex electro-mechanical systems. In the present work a Simulink model of the gyro-accelerometer system has been built using behavioral building blocks and behavioral simulations are executed to analyze the frequency response and transient behavior of the system. The mechanical part of the Simulink model is interfaced with suitable blocks and circuits for discrimination of acceleration and gyro action that occur simultaneously in the gyro-accelerometer output. With a given value of mass, spring stiffness and damping coefficient, the characteristic equations of motion expressed in *s*-domain can be easily solved by Simulink model in a few minutes.

***Index Terms*—**MEMS, Gyro-accelerometer, Simulink.

I. INTRODUCTION

MEMS technology has emerged as one of the most promising technology over the past few years and has attracted researchers from all parts of the globe [1, 2]. The world of MEMS has witnessed great advancements with continual development and has become a subject of interest in various science and engineering disciplines, as a multidisciplinary domain. Today, MEMS technology finds applications in various fields, few of them being aerospace, defence, automotive, biotechnology, telecommunication, consumer products, environmental protection and safety etc. Inertial MEMS form a major proportion of the MEMS market. Gyroscope and accelerometer represent two important categories of inertial technology for detecting motion [1]. There has been an exponential rise in the development of Inertial Measurement Units (IMUs) in recent years. This kind of a catastrophic development has taken place due to the availability of computer numerical algorithms which allow the designer to simulate multiple scenarios and optimize the design. The designs are taken up for fabrication only after thorough design analysis and verification, hence reducing the design-to-production time and cost drastically. Some of the commonly used techniques are the Finite Element Analysis based on Partial differential equations (pde's) and behavioral simulations based on *s*-parameter extraction.

The usual trend that is followed for simulations is the top down approach. Finite Element Analysis is a widely accepted technique for simulating the behavior of various mechanical structures. FEA is based on FEM (Finite Element Method) and hence is an accurate way of carrying out engineering analyses. One major drawback of FEM analyses is its intensive computational time and resource requirement. Simulation time depends on the type of physics, boundary conditions and the complexity of structures which makes it an extremely time consuming process to run optimization studies. On the other hand, behavioral simulations are a quick and easy way to simulate the response of complex structures to get a first cut solution [3]. With a given value of mass, spring stiffness and damping coefficient, the characteristic equations of motion can be easily solved by Simulink model in a few minutes as against FEM analysis that may take hours, days or even weeks together. Devices such as gyroscopes and gyro-accelerometer require more than one transient input for simulation. It is undoubtedly a cumbersome and time consuming procedure in FEM while the same analysis can be easily simulated in Simulink environment using suitable blocks and functions.

In our previous paper [4] reported, analytical modeling of the 2-DOF drive and 1-DOF sense gyro accelerometer structure has been presented. In the present paper, Simulink model of the gyro-accelerometer system has been built using behavioral building blocks and behavioral simulations are executed to analyze the response of the system.

II. MODEL

The structural configuration of the 2-DOF drive and 1-DOF sense mode capacitive gyro-accelerometer is shown in Fig. 1. It consists of two masses m_1 and m_2 bearing comb fingers with an intermediate frame mass m_f. The structure is set into excitation by applying a sinusoidal electrical excitation to the outer mass m_1, which causes the frame mass and mass m_2 to move together. The arrangement of flexures constrains the movement of mass m_1 in the sense direction. The second mass, m_2, is free to oscillate both in the drive and sense directions. Thus, m_2 forms the secondary mass of the 2-DOF drive mode oscillator. Masses m_f

and m_2 act as vibration absorber of m_1. The function of the frame mass m_f is to decouple the drive and sense modes in order to minimize dynamical coupling. By nesting m_2 inside a drive-mode frame, the sense-direction oscillations of the frame are constrained, and drive-direction oscillations are automatically forced to be in the designed drive direction. The second mass, m_2, is free to oscillate only in the sense-direction with respect to the frame. In the sense-direction, m_2 forms a resonant 1-DOF oscillator. Thus, in the presence of an input angular rate and linear acceleration, the Coriolis force is induced on m_2, and only m_2 responds to both the Coriolis force and linear acceleration. Equations of motion for the system are given below.

$$m_1\ddot{x}_1 + c_{1x}\dot{x}_1 + k_{1x}x_1 = k_{2x}(x_2 - x_1) + F_d(t), \quad (1)$$

$$(m_2 + m_f)\ddot{x}_2 + c_{2x}\dot{x}_2 + k_{2x}(x_2 - x_1) = 0, \quad (2)$$

$$m_2\ddot{y}_2 + c_{2y}\dot{y}_2 + k_{2y}y_2 = -2m_2\dot{x}_2\Omega_z - m_2x_2\dot{\Omega}_z + \mathcal{R}_{ex}, \quad (3)$$

where Ω_z is the angular rate around its z-axis of the device, $F_d(t) = F_o \sin \omega_d t$ is the driving electric force applied to drive mass m_1 with driving frequency ω_d. Coriolis force, $2m_2\dot{x}_2\Omega_z$, that excites mass m_2 in sense direction is responsible for the angular rate detection. $x_2\dot{\Omega}_z$ are the Euler's accelerations. The notations, c_{1x}, c_{2x} and c_{2y} are the damping constants, k_{1x}, k_{2x} and k_{2y} are the spring constants as shown in Fig.1. $\mathcal{R}_{ex}$ is the acceleration component has been taken into account for the analysis of gyro-accelerometer system.

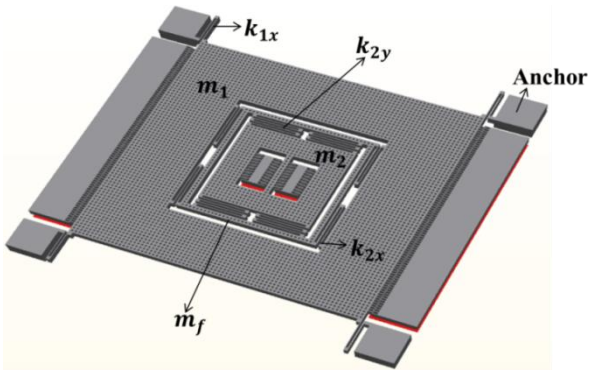

Fig.1 Conceptual schematic of the non-resonant gyro-accelerometer.

III. MATLAB/ SIMULINK MODEL AND SIMULATION RESULTS

The Simulink model is designed using the equations of motion of passive mass, $(m_f + m_2)$ and sense mass by expressing them in *s*-domain. The schematic of the model is depicted in Fig. 2. The model consists of a mechanical portion and demodulator portion. As explained in the previous section, masses m_f and m_2 together form a dynamic vibration absorber of the drive mass m_1, hence the mechanical portion of the simulink model is implemented by using the Eqs.2 and 3 only. These equations are expressed in *s*-domain with the acceleration terms isolated. The sense output signal,$\bar{y}_2(t)$ is modulated to the input signal and is the combined output of gyro-action and linear acceleration. In order to separate the combined output signal $\bar{y}_2(t)$and to demodulate it from the input signal, it is fed to the synchronous demodulation portion. The synchronous demodulation technique yields the in-phase and quadrature components that are given by $\bar{y}_p = \bar{y}_2(t)\cos(\omega t)$ and $\bar{y}_q = \bar{y}_2(t)\sin(\omega t)$ respectively. These signals have double frequency terms and have to be filtered out. For this purpose, Butterworth low pass filter is used. And finally the right hand side block is used for output measurement. The following table shows the parameters used for Simulink model designing.

Table 1: Parameter values used for calculations

Parameters	Values
Active mass (m_1)	111.33e-9 kg
Sense mass (m_2)	16.0381e-9 kg
Frame mass (m_f)	6.2281e-9 kg
Spring constant (k_{1x})	56.26 N/m
Spring constant (k_{2x})	14.06 N/m
Spring constant (k_{2y})	10.13 N/m
Operating Frequency	4 kHz
F_o	1.291e-5 N
Angular rate (Ω_o)	250 rad/s

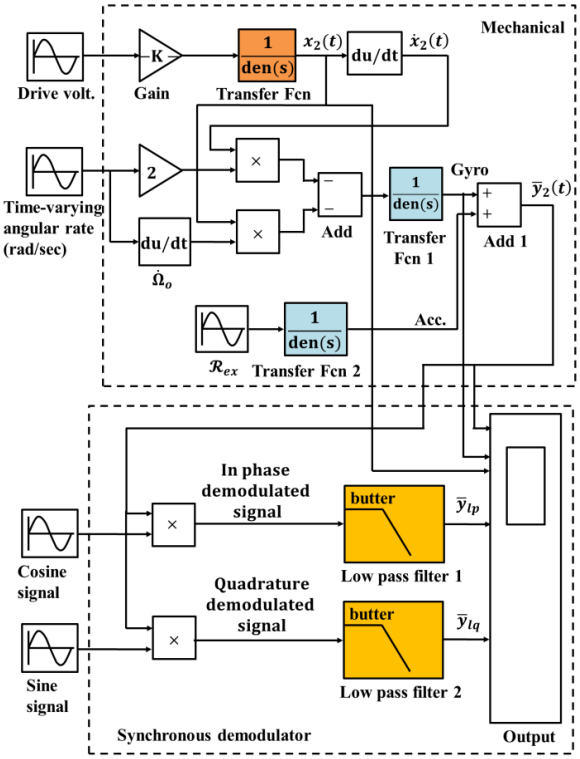

Fig. 2 Simulink model of a 2-DOF drive and 1-DOF sense gyro-accelerometer.

The operating frequencies for the passive drive mode and sense mode are obtained from the bode plot as illustrated in Fig. 3a, b.

Figure 4a-c shows the transient response of the model. Fig. 4a shows the passive mass displacement transient for $\lambda_{1x} = \lambda_{2x} = \lambda_{2y} = 50\ s^{-1}$ damping condition. From this figure it is clear that, at the beginning the amplitude is zero and as times passes, overall amplitude increases and after some time, gets saturated. It means, the device takes certain time for stabilization.

The variation of sense mass, m_2, displacement at an angular rate is shown in Fig. 4b. It is evident from the figure that the angular rate results in lobed characteristic. These displacement packets in terms of lobes arise due to the modulation of excited mode oscillation, which have been transferred to the sense mode caused by Coriolis force. Since, the angular rate is harmonic in nature with certain frequency, the repetition time period is a result of the same frequency. The first displacement packet occurs for shorter period compare to other lobes. This is, because; in starting moments the damping factor increases the repetition frequency. As a result of which, duration reduces.

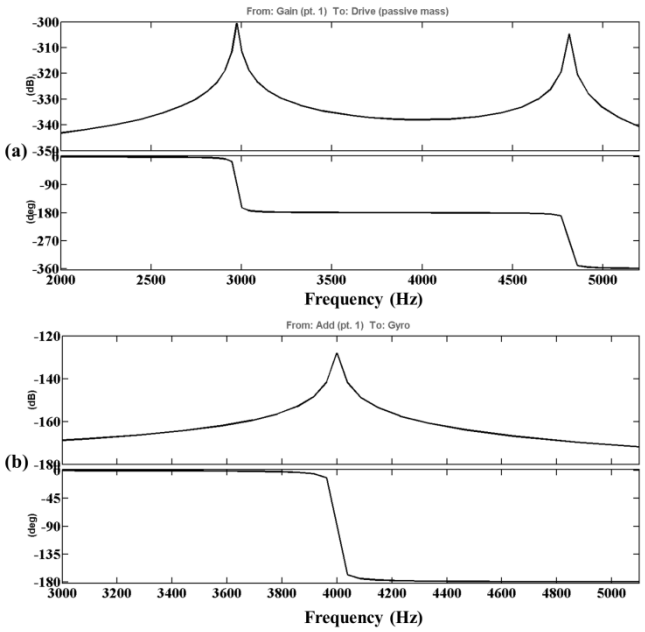

Fig. 3 Bode plot, (a) passive drive mode, (b) sense mode.

Figure 4c shows the combined effect of angular rate and linear acceleration on sense mode displacement. From this figure, it is clear that some value of linear accelerations causes the increase in the amplitude of mechanical oscillations and corresponding displacement packets are observed in sense mode as a result of Coriolis force.

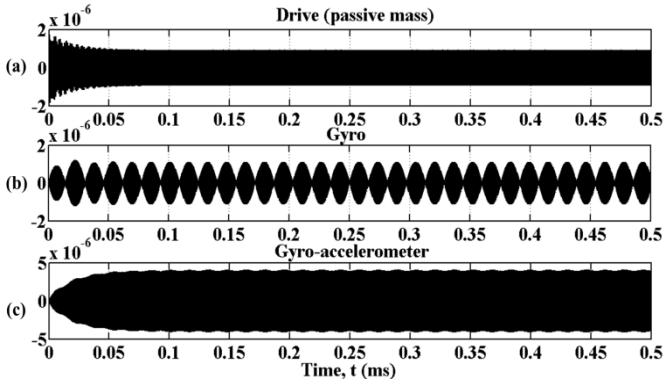

Fig. 4 Transient response at 4kHz operating frequency; (a) passive drive mass, (b) angular response of sense mass, (c) combined gyro-accelerometer response of sense mass.

Figure 5a shows the transient response of the in-phase component as a result of combined action of gyro and acceleration, after demodulation and filtration. The device settles down at about $0.1\ ms$ under damping conditions of $\lambda_{1x} = \lambda_{2x} = \lambda_{2y} = 50\ s^{-1}$. The settling time may vary depending upon the pressure conditions as in the case of vaccum shielded devices which require more time to settle down due to undamped condition. It is evident from the

in-phase plot, the acceleration action is dominant and the gyro action is insignificant, indicated by a straight line. Hence, acceleration can be measured through the in-phase output

Figure 5b shows the transient response of the quadrature component of displacement as a result of combined action of gyro and acceleration, after demodulation and filtration. It is evident from the quadratureplot, the gyro action is dominant and the acceleration action is insignificant, indicated by a sinusoidal variation. Hence, gyro action can be determined from the quadrature output.

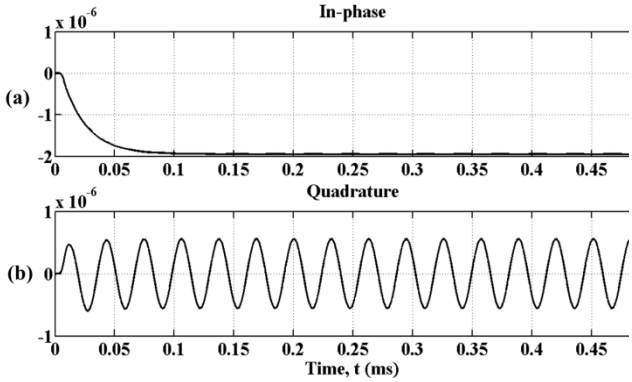

Fig. 5 Demodulated response, (a) in-phase output signal, $\bar{y}_{lp}$, (b) quadrature output signal, $\bar{y}_{lq}$.

IV. Conclusion

The gyro-accelerometer structure is represented by a behavioral model using suitable blocks from the electromechanical library in Simulink. The model is built using the equations of motion expressed in *s*-domain. Behavioral simulations are executed to analyze the frequency response and transient behavior of the system. The output of the system was subjected to synchronous demodulation in order to separate the gyro-action and linear those occur simultaneously in the gyro-accelerometer output. The dynamic analysis of gyro-accelerometer predicts that the output signal, after demodulation and filtration has in-phase and orthogonal components.The transient simulation was executed using ODE solver with a sampling rate of 10^{-6}seconds and was completed in about 30 seconds, which is an order faster than FEM analysis.

References

[1] N. Yazdi, F. Ayazi, K. Najafi, "Micromachined inertial sensors", in: Proceedings of the IEEE, vol. 86, no. 8, pp. 1640-1659, 1998.

[2] J. Soderkvist, "Micromachined gyroscopes", Sens. Actuat. A: Phys, vol. 43, pp. 65-71, 1994.

[3] M. Saukoski, "System and circuit design for a capacitive MEMS gyroscope", Ph.D. dissertation, Helsinki University of Technology, Finland, 2008.

[4] P. Verma, R. Gopal, S.K. Arya, "Analytical modeling and simulation of a 2-DOF drive and 1-DOF sense gyro-accelerometer", MicrosystTechnol, vol. 19, pp.1239-1248, 2013.